

2006

# Liquid-Flooded Ericsson Cycle Cooler: Part 1 – Thermodynamic Analysis

Jason Hugenroth  
*Purdue University*

James Braun  
*Purdue University*

Eckhard Groll  
*Purdue University*

Galen King  
*Purdue University*

Follow this and additional works at: <http://docs.lib.purdue.edu/iracc>

---

Hugenroth, Jason; Braun, James; Groll, Eckhard; and King, Galen, "Liquid-Flooded Ericsson Cycle Cooler: Part 1 – Thermodynamic Analysis" (2006). *International Refrigeration and Air Conditioning Conference*. Paper 823.  
<http://docs.lib.purdue.edu/iracc/823>

This document has been made available through Purdue e-Pubs, a service of the Purdue University Libraries. Please contact [epubs@purdue.edu](mailto:epubs@purdue.edu) for additional information.

Complete proceedings may be acquired in print and on CD-ROM directly from the Ray W. Herrick Laboratories at <https://engineering.purdue.edu/Herrick/Events/orderlit.html>

# LIQUID-FLOODED ERICSSON CYCLE COOLER: PART 1- THERMODYNAMIC ANALYSIS

Jason HUGENROTH<sup>1,\*</sup>, Jim BRAUN<sup>2</sup>, Eckhard GROLL<sup>3</sup>, Galen KING<sup>4</sup>

Purdue University, Mechanical Engineering, Herrick Laboratories  
West Lafayette, Indiana, USA

<sup>1</sup>[jhugenro@purdue.edu](mailto:jhugenro@purdue.edu)

<sup>2</sup>[jbrown@purdue.edu](mailto:jbrown@purdue.edu)

<sup>3</sup>[groll@purdue.edu](mailto:groll@purdue.edu)

<sup>4</sup>[kinggb@purdue.edu](mailto:kinggb@purdue.edu)

\*Corresponding author

## ABSTRACT

A novel implementation of a gas Ericsson cycle heat pump is presented. The concept uses liquid flooding of the compressor and expander to approach isothermal compression and expansion processes. A thermodynamic analysis of the cycle was performed using an EES-based computer model. In the ideal case with reversible components, the coefficient of performance (COP) of the cooler approaches the Carnot COP as the liquid flooding is increased. However, in the nonideal case when the rotating machinery operates irreversibly, there is an optimal liquid flooding rate and pressure ratio that produces the best performance. As with all gas cycles, the performance of the liquid flooded Ericsson cycle cooler is very sensitive to the efficiency of the compressor and expander. Results for two cycle configurations are presented.

## 1. INTRODUCTION

A cooling mode Ericsson cycle heat pump (i.e. Ericsson cycle cooler) was explored as an alternative to vapor compression systems. The motivation of the work was the elimination of HFC refrigerants, which are potent greenhouse gases. Gas cycles, such as the Ericsson cycle, can use environmentally benign gases as working fluids, such as air, argon, xenon, or helium. Replacement of HFC refrigerants with natural working fluids would reduce the direct impact of refrigerant leakage on global warming. However, in order to not increase the indirect global warming impact due to burning of fossil fuels for electricity generation, alternatives to vapor compression systems should have equal or better operating efficiencies.

The liquid flooded Ericsson cooler (LFEC) is a modification of the basic reverse Ericsson cycle that overcomes the substantial practical difficulties of achieving isothermal compression and expansion processes. In this case, isothermal compression and expansion is approached by mixing a nonvolatile liquid with the noncondensable gas during the compression and expansion processes. The term “flooded” comes from the notion that the compressor and expander are flooded with large quantities of liquid. Liquid mass flow rates may be significantly greater than gas flow rates. This is in contrast to oil injection schemes in some types of positive displacement compressors where the principle purpose is to improve sealing of the leakage paths and the reduction of friction within the compressor, and the oil flow rates represent only about 1% to 5% of the total flow by mass.

If the liquid’s capacitance rate (liquid specific heat times the liquid mass flow rate) is much greater than the gas’ capacitance rate most of the heat of compression of the gas can be absorbed by the liquid. In the limiting case where the ratio of liquid to gas capacitance rate is infinite and perfect thermal contact between the gas and the liquid are assumed, isothermal compression and expansion will be achieved. As with the basic Ericsson cycle, the COP for the ideal LFEC is the Carnot COP.

Since the LFEC cycle has not been studied previously most of the work presented represents new contributions to the literature. However, a literature review revealed some prior work that was relevant to the research presented here. A brief summary of the literature review follows.

Corey (1990) developed a concept that is schematically similar to the LFEC. Corey's (1990) concept was tested but failed to produce a net heat pumping effect. A thermodynamic analysis of the cycle was not presented. Several examples exist in the literature (e.g. Hiwata et al., 2002) where oil flooding is used in scroll or screw compressors to seal leakage paths within the compressor. Often, the ability of the oil to absorb the heat of compression was not considered these works. One exception is a paper by Elson and Butler (2003) on the use of an oil flooded scroll compressor for application to high heat of compression gases. In their work, the oil was specifically used to absorb the heat of compression for gases with high ratios of specific heats. However, no theoretical development or relevant experimental results were presented.

Several factors prevent the LFEC from operating in the ideal sense. Finite capacitance rates lead to non-isothermal compression and expansion, which results in heat transfer irreversibilities in the external heat exchangers required for the cycle. Additional irreversibilities arise due to imperfect thermal contact between the liquid and the gas during the compression and expansion processes, which implies irreversible heat transfer. As with all gas cycles, the flooded Ericsson cycle is very sensitive to inefficiencies that exist in real compressors and expanders.

Two configurations for the liquid flooded Ericsson cycle cooler (LFEC) are shown in Figures 1 and 2. These differ by the location of the heat exchangers in the system. The type 1 (LFEC 1), shown in Figure 1, has the heat exchangers placed in the liquid streams after the liquid and gas have been separated. The type 2 (LFEC 2), shown in Figure 2, has the heat exchangers immediately downstream of the compressor and expander before the gas and liquid are separated. It will be shown that the LFEC 2 configuration outperforms the LFEC 1 configuration, when nonideal operation is considered.

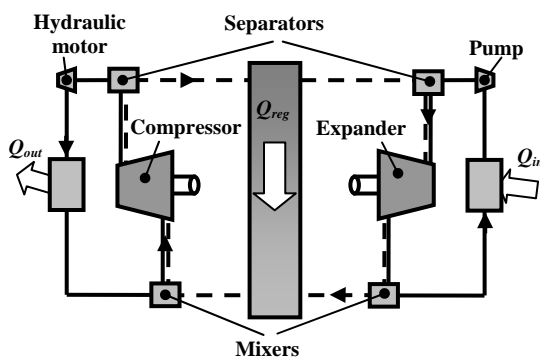


Figure 1: Schematic of Type 1 liquid flooded Ericsson Cooler (LFEC 1)

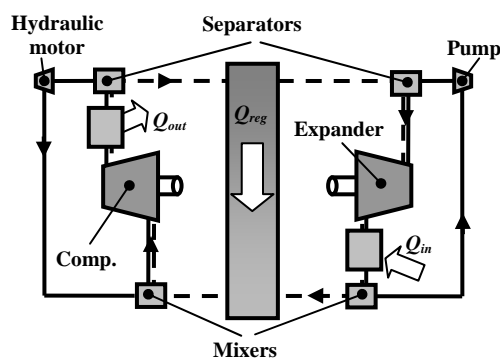


Figure 2: Schematic of Type 2 liquid flooded Ericsson Cooler (LFEC 2)

This paper presents the development of an idealized LFEC model including the development of an analytical model for liquid flooded compression. Modeling results for liquid flooded compression are presented followed by the modeling results for the LFEC 1 cycle. A performance comparison between the LFEC 1 and LFEC 2 configurations is also included. The results are summarized on the Summary section of this paper.

## 2. IDEAL FLUID LIQUID FLOODED ERICSSON COOLER MODEL

An ideal fluid LFEC model was developed and used to explore the behavior of the liquid flooded Ericsson cycle cooler. The simple model makes use of the following simplifying assumptions:

- Constant specific heats for the gas and liquid
- Ideal gas
- Incompressible, nonvolatile liquid
- No pressure drops
- All components operate adiabatically (except the heat exchangers)
- Perfect separation

- Perfect mixing
- Combined liquid and gas flows are in thermal equilibrium

## 2.1 Liquid Flooded Compressor and Expander Model

An analytical compressor model was developed by examining the behavior of an ideal gas that is in contact with a liquid and defining for properties of a pseudo-gas that characterizes the mixture. Using these effective properties, standard thermodynamic relations can be used to determine the compression power and temperature change for the gas as it is compressed.

Considering a rigid sealed container that contains a liquid and a gas, where heat is added to the mixture in the container, the first law of thermodynamics can be expressed as follows:

$$\delta Q = dU = m_g du_g + m_l du_l \quad (1)$$

Since  $du$  is defined as,

$$du = c_v dT \quad (2)$$

Equation (1) becomes,

$$dU = m_g c_{v,g} dT + m_l c_l dT \quad (3)$$

where,

$$dU = m_g du^* \quad (4)$$

This leads to,

$$du^* = c_{v,g}^* dT = \frac{m_g c_{v,g} dT + m_l c_l dT}{m_g} \quad (5)$$

or,

$$c_{v,g}^* = \frac{m_g c_{v,g} + m_l c_l}{m_g} \quad (6)$$

where  $c_{v,g}^*$  is termed the effective constant volume specific heat and is the average specific heat of the liquid and the gas weighted by the liquid and gas masses. Following the same approach, the effective constant pressure specific heat is

$$c_{p,g}^* = \frac{m_g c_{p,g} + m_l c_l}{m_g} \quad (7)$$

The isentropic exponent or ratio of specific heats for an ideal gas is defined as

$$k = \frac{c_{p,g}}{c_{v,g}} \quad (8)$$

By dividing Equation (7) by Equation (6) the effective ratio of specific heat is

$$k^* = \frac{m_g c_{p,g} + m_l c_l}{m_g c_{v,g} + m_l c_l} \quad (9)$$

Specific heats are also related to the gas constant  $R$  by

$$R = c_p - c_v \quad (10)$$

Similarly an effective gas constant for a gas in contact with liquid can be defined as

$$R^* = c_{p,g}^* - c_{v,g}^* \quad (11)$$

However,

$$c_{p,g}^* - c_{v,g}^* = c_p - c_v \quad (12)$$

which is easy to see from inspection of Equations (6) and (7). Therefore, the effective gas constant  $R^*$  is equal to the ideal gas constant  $R$ . For an internally reversible steady flow device, the specific work is found by integrating

$$w = \int_{P_i}^{P_o} v dP \quad (13)$$

from the initial pressure  $P_i$  to the final pressure  $P_o$ . An ideal gas with a constant specific heat ratio of  $k$  that is undergoing a compression process in thermal equilibrium with an incompressible liquid having a constant specific heat behaves exactly like an ideal gas having a constant specific heat equal to  $k^*$ . Therefore, the result of integrating equation (13) for the cooled ideal gas is the same as that for adiabatic reversible work of an ideal gas with  $k^*$  substituted for  $k$ . The result is

$$w_g = \frac{RT_i k^*}{k^* - 1} \left[ \frac{P_o^{k^*}}{P_i^{k^*}} - 1 \right] \quad (14)$$

where  $w_g$  is the specific reversible work required to compress the gas that is in thermal equilibrium with a liquid and  $P_{ratio}$  is the ratio of  $P_o$  to  $P_i$ . The reversible work required to pump the incompressible liquid is

$$w_l = v(P_o - P_i) \quad (15)$$

Equation (15) neglects the relatively small impact of temperature changes on specific volume of the liquid.

The total reversible compressor power is,

$$\dot{W}_{ideal} = \dot{m}_g w_g + \dot{m}_l w_l \quad (16)$$

This expression is positive for a liquid gas mixture that is being compressed. For an expander, the sign changes on the right hand sides of Equations (14), (15), and (16) indicating that work out is negative. This is consistent with the convention adopted here that all energy flows into a control volume are positive and all energy flows out are negative.

Similar to the reversible work, the temperature change for the gas during a reversible flooded compression process is found by substituting  $k^*$  for  $k$  in the conventional isentropic relations for ideal gases, resulting in

$$\frac{T_{o,ideal}}{T_i} = P_{ratio}^{\frac{k^*-1}{k^*}} \quad (17)$$

where,  $T_{o,ideal}$  is the ideal outlet temperature for a flooded compressor or expander process.

The actual compression power for the gas and liquid mixture is determined using an adiabatic efficiency defined as

$$\eta_c \equiv \frac{\dot{W}_{ideal}}{\dot{W}_{actual}} \quad (18)$$

where  $\dot{W}_{ideal}$  is the adiabatic and reversible (i.e., isentropic) liquid flooded compressor power and  $\dot{W}_{actual}$  is the actual liquid flooded compressor power. For a liquid flooded expander, the adiabatic efficiency is the reciprocal of Equation (18) or

$$\eta_e \equiv \frac{\dot{W}_{ideal}}{\dot{W}_{actual}} \quad (19)$$

For an adiabatic steady flow device, liquid flooded compression or expansion power can also be written as

$$\dot{W}_{actual} = \dot{m}_g c_p (T_o - T_i) + \dot{m}_l c_l (T_o - T_i) + \dot{m}_l v (P_o - P_i) \quad (20)$$

Once the actual compressor or expander power is known, Equation (20) can be used to determine the actual outlet temperature.

## 2.2 Modeling of the Remaining Components in the System

The remaining components in the LFEC model include hot and cold side heat exchangers, a regenerator, hot and cold side mixers, hot and cold side separators, a hydraulic motor, and a pump.

Effectiveness models were used for the heat exchangers. It was assumed that the minimum capacitance rate across the heat exchangers corresponded to the refrigerant-side flows, as opposed to the air-side flows. This means that at an effectiveness value of 1.0, the temperature of the refrigerant flow exiting the heat exchanger would be equal to the inlet air temperature. The temperature of the liquid and gas exiting the separators is assumed to be equal to the fluid inlet temperature. The mixer model implements an adiabatic mixing process. The pump and hydraulic motor power were determined by multiplying the specific work (Equation (15)) by the mass flow rate of the liquid. Adiabatic efficiencies were applied to these components to account for non-ideal operation.

## 3. IDEAL FLUID FLOODED ERICSSON COOLER MODEL RESULTS

The modeling results for the LFEC model are discussed in the following sections. Results for flooded compression as a stand-alone component are shown first, followed by an analysis of the LFEC 1 configuration. Lastly, a brief comparison of the LFEC 1 and LFEC 2 configurations is made.

### 3.1 Ideal Gas Flooded Compression and Expansion Model

The behavior of a liquid flooded compressor or expander differs from dry compression or expansion. Therefore, it is useful to explore their behavior as independent components before investigating the entire cycle. Since flooded expansion is analogous to flooded compression, results will only be shown with respect to the compression process. In the analysis that follows, the working fluids were nitrogen and alkyl-benzene oil and model inputs shown in Table 1 were used, unless otherwise specified. In Table 1,  $\dot{V}_{total}$  is the compressor displacement rate, which is defined as the displacement volume times the shaft speed in Hertz.

Table 1: Input parameters for flooded compression modeling.

$T_i$ (°C)	$P_i$ (kPa)	$P_{ratio}$	$\eta_c$	$\dot{V}_{total}$ (cm <sup>3</sup> /s)	$k$
30.0	500	2.5	1.0	6000	1.4

Several figures are plotted against the capacitance rate ratio ( $C_{ratio}$ ), which is defined as

$$C_{ratio} \equiv \frac{\dot{m}_l c_l}{\dot{m}_g c_{p,g}} \quad (21)$$

This convenient parameter eliminates the need to consider the flow rates and specific heat values of the fluids independently.

Figure 3 shows nondimensional compressor discharge temperature and the effective ratio of specific heats as a function of  $C_{ratio}$ . The discharge temperature was nondimensionalized with respect to the compressor inlet temperature. The effective isentropic exponent and discharge temperature approach 1.0 as  $C_{ratio}$  increases. The slopes of the curves are very steep for  $C_{ratio}$  values less than about 30. For oil circulation rates of 1% liquid flow rate by volume,  $C_{ratio}$  is equal to about 3 and  $k^*$  is about 1.08.

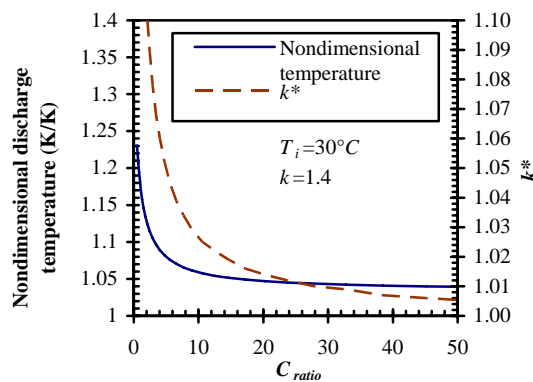


Figure 3: Nondimensional compressor discharge temperature and  $k^*$  as a function of  $C_{ratio}$ .

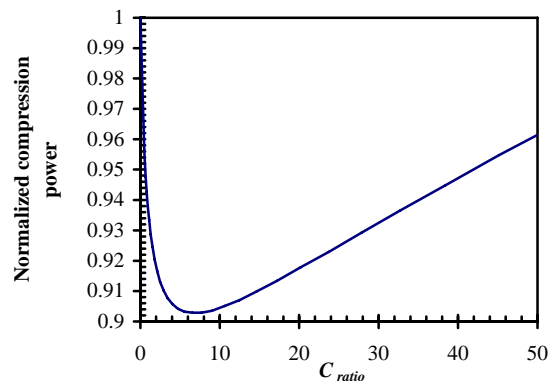


Figure 4: Normalized compressor power as a function of  $C_{ratio}$ .

For a dry reversible isothermal compression process, the compression power is much smaller than in the adiabatic case. For flooded compression, as  $C_{ratio}$  increases (i.e. the liquid injection rate increases) the process becomes more isothermal and gas compression work decreases. However, the work required to pump the liquid increases with  $C_{ratio}$  and there is an optimal  $C_{ratio}$  that minimizes compression work. This minimum is illustrated in Figure 4 where the normalized compression power is shown as a function of  $C_{ratio}$ . The compression power reaches a minimum at a  $C_{ratio}$  of about 7 where a little over 90% of the total possible change in  $k^*$  has occurred. At higher liquid flow rates, further reductions in gas compression work are more than offset by an increase in liquid pumping work. The results shown in Figure 4 were for a compressor with a fixed displacement rate. Therefore, as the liquid flow rate increased the gas flow rate decreased. However, if the gas flow rate was fixed by varying the displacement rate, a minimum in compressor power curve would still occur.

### 3.2 Ideal Fluid Model Results for the Liquid Flooded Ericsson Cooler

This section presents ideal fluid modeling results for the LFEC. Most of the results are presented with respect to the LFEC 1 configuration, but comparisons between the LFEC 1 and LFEC 2 configurations are also presented. Cycle behavior with ideal components is considered first, followed by analysis of the impact of component irreversibilities on performance. In order to generalize the results, capacity was divided by the compressor displacement rate resulting in units of energy per unit volume. This volumetric capacity is defined as

$$q_v \equiv \dot{Q}/\dot{V} \tag{22}$$

The use of volumetric capacity makes the results of the analysis independent of the physical size of the equipment. Unless otherwise specified the inputs used in Table 2 were used.

Table 2: Input parameters for ideal gas LFEC 1 modeling.

$T_{ref}$ (°C)	$T_\infty$ (°C)	$P_i$ (kPa)	$P_{ratio}$	$\rho_l$ (kg/m <sup>3</sup> )	$c_l$ (J/kg-K)	$c_p$ (J/kg-K)	$k$
2.0	32.2	500	2.5	850	1800	1040	1.4

Figure 5 shows second law efficiency (i.e. COP/COP<sub>carnot</sub>) and volumetric capacity as a function of  $C_{ratio}$ , when all rotating machinery has 100% isentropic efficiencies and all heat exchangers have effectiveness values of 1.0. Although the  $C_{ratio}$  values for the hot and cold side liquid loops can be different, they were made equal for the results of Figure 5. The second law efficiency increases and approaches unity as  $C_{ratio}$  increases because greater liquid flow through the compressor and expander leads to smaller temperature changes. The nonideal performance at low liquid flooding rates comes from two sources, one internal and one external. The external irreversibility is due to heat rejection and addition across a finite temperature difference. The internal irreversibility results from the mixing of the liquid and gas at two different temperatures. This occurs before the fluid mixture enters the compressor and expander. The nonisothermal compression and expansion processes themselves are reversible. However, the temperature changes of the liquids across the compressor and expander result in temperature changes across the heat exchangers, resulting in heat transfer irreversibilities.

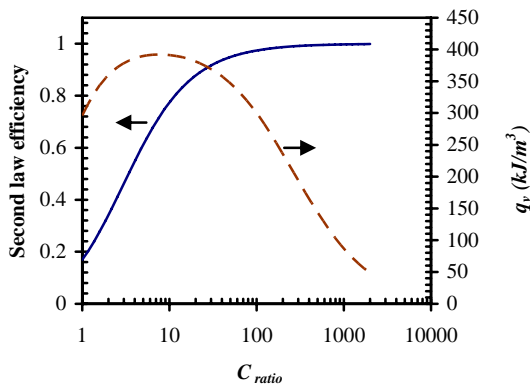


Figure 5: LFEC 1 second law efficiency and volumetric capacity as a function of  $C_{ratio}$  when all components are ideal.

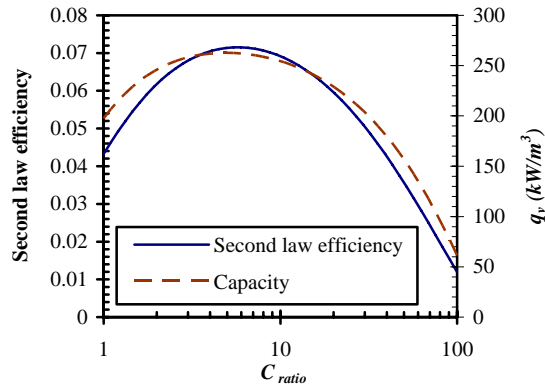


Figure 6: LFEC 1 second law efficiency and volumetric capacity as a function of  $C_{ratio}$  with  $\eta = 0.70$  for the rotating machinery.

In Figure 5, the volumetric capacity (dashed line) first increases and then drops asymptotically to zero as  $C_{ratio}$  increases. The cooling capacity is the product of the cold liquid mass flow rate and the inlet and outlet liquid temperature differential for the cold heat exchanger. Increasing  $C_{ratio}$  causes an increase in cold liquid flow rate, but a reduction in the temperature differential. The peak capacity occurs at a point where the product of these two quantities is maximum and is not related to the compressor power minimum or expander power maximum that were described earlier. As the liquid flow approaches infinity, the cycle COP approaches Carnot COP but with zero cooling capacity.

For the case where the rotating machinery operates irreversibly, the cycle performs qualitatively much differently than for ideal components. Figure 6 shows second law efficiency as a function of  $C_{ratio}$  for  $\eta = 0.7$  applied to the

compressor, expander, hydraulic motor, and pump. Similar to other gas cycles, the performance is very sensitive to the adiabatic efficiency of the rotating machinery. Even for  $\eta = 0.95$  (not shown), the best second law efficiency is less than 40%, for the specified source and sink temperatures. In contrast to the ideal cycle performance, there is an optimal liquid flow rate that results in peak cycle efficiency. Although not shown here, the optimal  $C_{ratio}$  decreases as  $\eta$  decreases. Volumetric capacity is also shown in Figure 6 as a function of  $C_{ratio}$ . Although the variation of capacity with  $C_{ratio}$  is qualitatively similar to the ideal case, the capacity decreases substantially as  $\eta$  decreases.

The high sensitivity of LFEC performance to compressor and expander efficiencies is a characteristic of all gas cycles. This occurs because the compressor power required per unit capacity is large for gas cycles, in comparison to vapor compression cycles operating under similar conditions. Since the required compressor power for gas cycles is relatively large, irreversible compressor operation has a significant impact on the cycle performance. In addition, losses that occur in the expander of gas cycles contribute further to this sensitivity.

In the earlier analysis, dealing strictly with liquid flooded compression, it was shown that a certain amount of liquid flooding would minimize the required compressor power. By analogy it is also the case that a certain amount of liquid flooding will maximize the expander power output. However, it is not the case that the optimum cycle efficiency corresponds to the power minimum and maximum of the compressor and expander, respectively. In fact, the optimum  $C_{ratio}$  value for the compressor and expander in the system is greater than the optimum value for these components operating independently. However, as the adiabatic efficiency of the compressor and expander decreases, the optimum system  $C_{ratio}$  values for these components tend toward the optimum  $C_{ratio}$  values of the compressor and expander operating as stand alone components.

It has been established that when the rotating machinery in the cycle operates irreversibly there is a specific amount of liquid flooding that optimizes cycle efficiency. There are, however, still a number of parameters that have not been considered in the cycle optimization. These include pressure ratio, nominal system pressure, system working fluids, and independent  $C_{ratio}$  values for the compressor and expander. Space constraints preclude a detailed discussion of these additional parameters. However, additional optimization studies led to the following conclusions: 1) there is an optimum pressure ratio for the cycle, 2) optimum  $C_{ratio}$  values for the compressor and expander are different from one another, 3) cycle performance improves as the nominal system pressure decreases, and 4) other fluid combinations can lead to improved cycle performance.

The effect of operating temperatures on performance was also considered. While the sink and source temperatures can both vary, the primary objective is to explore the variation in performance with source temperature. This is because the required source temperature is determined by the particular application. This can vary from human comfort cooling, where the temperature lift is fairly small, to cryogenics, where the lift is large.

Figure 7 shows how second law efficiency varies with source temperature for a constant sink temperature of 32.2°C for the LFEC 1 configuration. The adiabatic efficiencies for the rotating machinery and effectiveness values for the heat exchangers and regenerator were set to 0.80. The corresponding optimum pressure ratio and  $C_{ratio}$  values are also plotted in Figure 7. The performance peaks at about -85°C. Cascade vapor compression systems are commonly employed in applications that require temperatures in this range (e.g. laboratory freezers). The LFEC offers a potential efficiency improvement compared to these types of systems and uses environmentally benign refrigerants. Also, the complexity of the LFEC system, and presumably the cost, are similar to a cascade type vapor compression system. However when compared to simple vapor compression systems used for near ambient refrigeration applications, the LFEC is much more complicated.

A natural limitation on the source and sink temperatures for the LFEC are the boiling and freezing points of the flooding liquid. In principle, the liquid used on the hot and cold sides of the system are isolated and therefore can be different. In practice, there is liquid carryover through the regenerator due to incomplete separation in the separators. Preventing this would pose an engineering challenge. One possible working fluid for low temperature applications is ethanol. Ethanol has freezing and boiling points of -114.1°C and 78.5°C, respectively.

Figure 8 compares second law efficiencies for the LFEC 1 and LFEC 2 cycles as a function of  $T_{ref}$ , using nitrogen and alkyl-benzene oil. In general, the LFEC 2 cycle outperforms the LFEC 1 cycle when nonideal operation is assumed. Qualitatively, the behavior of the two configurations tends to be somewhat similar.

## 4. SUMMARY

A novel approach to implementing a gas Ericsson cycle heat pump was developed. The concept uses liquid flooding of the compressor and expander to approach isothermal compression and expansion processes. A thermodynamic analysis of the LFEC in two configurations was performed using a computer model. For ideal components, the COP of the cooler approaches the Carnot COP as liquid flooding is increased. However, when considering internal irreversibilities in the heat exchangers and rotating machinery, there is an optimum amount of liquid flooding and an optimum pressure ratio that maximize cycle COP. The cycle was found to have the highest second law efficiency at source temperatures in the range of  $-85^{\circ}\text{C}$  when heat is rejected to a sink at  $32.2^{\circ}\text{C}$

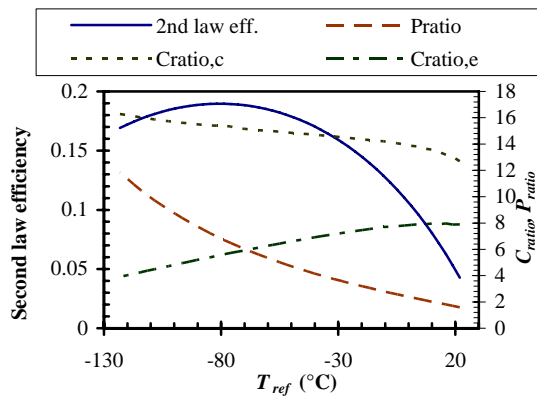


Figure 7: Second law efficiency and optimum  $C_{ratio}$  and  $P_{ratio}$  values for the LFEC 1 cycle as a function of  $T_{ref}$ .

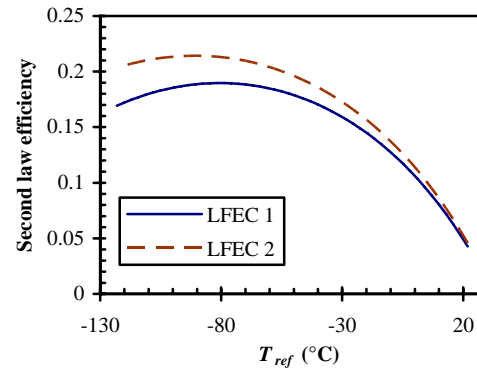


Figure 8: Comparison of LFEC 1 and LFEC 2 second law efficiencies as a function of  $T_{ref}$ .

## NOMENCLATURE

$Q$	Heat transfer	<b>Subscripts, Greek, and miscellaneous</b>	
$c$	Specific heat	$c$	Compressor
$C_{ratio}$	Capacitance rate ratio	$e$	Expander
$k$	Ratio of specific heats	$f$	Final
$m$	Mass	$g$	Gas
$\dot{m}$	Mass flow rate	$i$	In, initial
$P$	Pressure	$l$	Liquid
$P_{ratio}$	Pressure ratio	$o$	Out, final
$q_v$	Volumetric capacity	$ref$	Cold space
$T$	Temperature	$v$	Volume
$U$	Internal energy	$\infty$	Ambient
$u$	Specific internal energy	$*$	Effective
$v$	Specific volume	$\eta$	Adiabatic efficiency
$w$	Specific work		
$\dot{W}$	Power		

## REFERENCES

- Corey, J., 1990, "A Rotary Air-Cycle Refrigerator with Thermally-Active Liquid Pistons", *25<sup>th</sup> Intersociety Energy Conversion Engineering Conference*, Vol. 6, pp. 286-291.
- Elson, J. P., Butler, B. R., 2003, "A Hermetic Scroll Compressor for Application to High Heat-of-Compression Gases", *International Conference on Compressors and their Systems*, pp. 55-66.
- Hiwata, A., Iida, N., Futagami, Y., Sawai, K., 2002, "Performance Investigation with Oil-Injection to Compression Chambers on CO<sub>2</sub>-Scroll Compressor", *Proceedings of the 2002 International Compressor Engineering Conference at Purdue*, C18-4